Contribution from the Departments of Chemistry, University of Denver, Denver, Colorado 80208, and University of Colorado at Denver, Denver, Colorado 80202

Metal-Nitroxyl Interactions. 33. Single-Crystal EPR Spectra of Two Spin-Labeled Silver Porphyrins

REDDY DAMODER, KUNDALIKA M. MORE, GARETH R. EATON,* and SANDRA S. EATON

Received April 22, 1983

Single-crystal EPR spectra have been obtained for two spin-labeled silver porphyrins doped into zinc tetraphenylporphyrin. For each of the complexes four conformations were observed. The dependence of the electron–electron spin–spin splittings on the orientation of the crystal in the magnetic field was analyzed to obtain the isotropic exchange and anisotropic dipolar contributions to the interaction. The interspin distance, r, ranged from 9.5 to 13.8 Å. Values of the exchange coupling constant, J, ranged from -35×10^{-4} to $+7 \times 10^{-4}$ cm^{-1}. There was no correlation between the values of r and J. Comparison of the values of J obtained for the series of vanadyl, copper, and silver complexes of the spin-labeled porphyrins in fluid solution and frozen solution and those doped into ZnTPP indicated good agreement among the results obtained in the three media. Exchange increased in the order $V^{IV}O$ < Cu(II) < Ag(II) and was greater for the trans isomers than for the cis isomers.

Introduction

There is increasing awareness of the importance of electron–electron spin–spin interaction in biological systems. In bacterial systems, spin-coupled EPR spectra have been observed for one of the transient intermediates in the photosynthetic process.[1,2] The EPR spectrum of horseradish peroxidase compound I has been interpreted as arising from spin–spin coupling between a ferryl center ($S = 1$) and an organic radical ($S = {}^1/_2$).[3] Interaction between Co(II) and an organic radical has been observed in B_{12} coenzyme systems.[4-6] To aid in the interpretation of the results obtained for natural systems, it would be useful to understand the factors that contribute to variations in the magnitude of the interaction.

In general, weak electron–electron spin–spin interaction consists of an isotropic exchange interaction and an anisotropic dipolar interaction. Antisymmetric and anisotropic exchange can be neglected when the isotropic exchange is less than a few cm^{-1}. The dipolar splitting depends on the cube of the interspin distance r. The isotropic exchange coupling constant J depends on the overlap of the orbitals containing the unpaired electrons. For short interspin distances exchange results from direct overlap of the two orbitals. However, for longer interspin distances the overlap occurs indirectly through the intervening bonds. Thus the value of J depends on the nature of the bonding pathway and its conformation. To interpret spin–spin splittings in EPR spectra obtained in randomly oriented media (powder spectra or frozen-solution spectra), it is necessary to separate the exchange and dipolar terms. It would be helpful to have methods for separately determining or estimating the two contributions. We have recently shown that for two $S = {}^1/_2$ spins with g about 2 the relative intensity of the half-field transition can be used to determine the interspin distance.[7] For molecules that are rapidly tumbling in fluid solution, anisotropic contributions to the spin–spin splitting are averaged to approximately zero and only the isotropic exchange splittings are observed. However, the dependence of J on the molecular conformation raises the question as to whether values obtained for J in fluid solution can be used to estimate values for rigid-lattice spectra. We have therefore begun a series of studies to compare the values of J obtained from fluid-solution and rigid-lattice spectra of spin-labeled metal complexes. In a series of spin-labeled copper complexes the values of J obtained from frozen-glass spectra were in good agreement with values obtained in fluid solution.[8] In fluid solution it was observed that for the series of spin-labeled complexes I–V the values

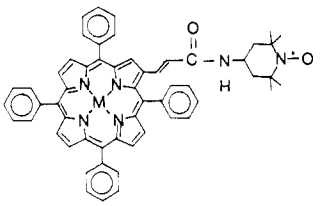

M	isomer	
Cu	trans	I
Cu	cis	II
VO	cis	III
Ag	trans	IV
Ag	cis	V

of J increased in the order $V^{IV}O$ < Cu(II) < Ag(II) and that exchange was greater for the trans isomers than for the cis isomers.[9] When I and II were doped into zinc tetraphenylporphyrin (ZnTPP), it was found that the values of J were strongly dependent on the molecular conformation, but the overall pattern still showed that exchange was greater through the trans linkage than through the cis linkage.[10] EPR spectra of III doped into ZnTPP confirmed the results obtained in fluid solution, that exchange was smaller for the vanadyl complex than for the analogous copper complex.[11] We have now examined the analogous silver complexes IV and V doped into ZnTPP, and the results are presented in this paper.

Experimental Section

The compounds studied here were prepared by literature methods: IV and V,[9] tetraphenylporphyrin,[12,13] and zinc tetraphenylporphyrin.[14] No EPR spectrum was observed for ZnTPP as a powder or as a single crystal. Tetrahydrofuran (THF) was dried over potassium ribbon, distilled, and stored in the dark. EPR spectra were obtained at room temperature on a Varian E-9 spectrometer. Data were collected digitally with a Varian 620/L-103 minicomputer and the CLASS language. To improve the signal-to-noise ratio of the spectra, mod-

(1) Blankenship, R. E. *Acc. Chem. Res.* **1981**, *14*, 163-170.
(2) Klimov, V. V.; Krasnovskii, A. A. *Photosynthetica* **1981**, *15*, 592-609.
(3) Schulz, C. E.; Devaney, P. W.; Winkler, H.; Debrunner, P. G.; Doan, N.; Chiang, R.; Hager, L. P. *FEBS Lett.* **1979**, *103*, 102-105.
(4) Schepler, K. L.; Dunham, W. R.; Sands, R. H.; Fee, J. A.; Abeles, R. H. *Biochim. Biophys. Acta* **1975**, *397*, 510-518.
(5) Buettner, G. R.; Coffman, R. E. *Biochim. Biophys. Acta* **1977**, *480*, 495-505.
(6) Boas, J. F.; Hicks, P. R.; Pilbrow, J. R.; Smith, T. D. *J. Chem. Soc., Faraday Trans. 2* **1978**, *74*, 417-431.
(7) Eaton, S. S.; Eaton, G. R. *J. Am. Chem. Soc.* **1982**, *104*, 5002-5003. Eaton, S. S.; More, K. M.; Sawant, B. M.; Eaton, G. R. *J. Am. Chem. Soc.*, in press.
(8) Eaton, S. S.; More, K. M.; Sawant, B. M.; Boymel, P. M.; Eaton, G. R. *J. Magn. Reson.* **1983**, *52*, 435-449.
(9) More, K. M.; Eaton, S. S.; Eaton, G. R. *J. Am. Chem. Soc.* **1981**, *103*, 1087-1090.
(10) Damoder, R.; More, K. M.; Eaton, G. R.; Eaton, S. S. *J. Am. Chem. Soc.* **1983**, *105*, 2147-2153.
(11) Damoder, R.; More, K. M.; Eaton, G. R.; Eaton, S. S. *Inorg. Chem.* **1983**, *22*, 2836-2841.
(12) Adler, A. D.; Longo, F. R.; Finarelli, J. D.; Goldmacher, J.; Assour, J.; Korsakoff, L. *J. Org. Chem.* **1967**, *32*, 476.
(13) Rousseau, K.; Dolphin, D. *Tetrahedron Lett.* **1974**, 4251-4254.
(14) Adler, A. D.; Longo, F. R.; Kampas, F.; Kim, J. *J. Inorg. Nucl. Chem.* **1970**, *32*, 2443-2444.

* To whom correspondence should be addressed at the University of Denver.

0020-1669/83/1322-3738$01.50/0

Table I. g and A Values for the Silver[a,b] and Nitroxyl Electrons

electron	compd	species	g_{xx}	g_{yy}	g_{zz}	A_{xx}[c]	A_{yy}[c]	A_{zz}[c]
silver	IV	1–4	2.040	2.040	2.110	26	28	53
silver	V	1–4	2.035	2.042	2.106	26	26	53
nitroxyl	IV	1	2.0082	2.0051	2.0040	9	9	27
nitroxyl	IV	2	2.0076	2.0066	2.0050	7	12	29
nitroxyl	IV	3	2.0082	2.0066	2.0030	7	10	29
nitroxyl	IV	4	2.0082	2.0055	2.0035	10	7	27
nitroxyl	V	1	2.0085	2.0055	2.0030	9	9	27
nitroxyl	V	2–4	2.0089	2.0066	2.0035	6	4	29

[a] The principal values of the porphyrin nitrogen hyperfine coupling tensor were $A_{xx} = 20.5 \times 10^{-4}$ cm^{-1}, $A_{yy} = 20.5 \times 10^{-4}$ cm^{-1}, and $A_{zz} = 25.5 \times 10^{-4}$ cm^{-1}. [b] Values are for ^{107}Ag. [c] In units of 10^{-4} cm^{-1}.

ulation amplitudes up to half the peak-to-peak line widths were used to obtain the spectra. Although the use of such large modulation amplitudes causes slight distortion of the line shape, it should have no impact on the apparent line positions and a negligible impact on the analysis of the spectra.

Single crystals were grown by slow evaporation (3–4 days) of a solution containing a 99:1 ratio by weight of ZnTPP:IV or ZnTPP:V in purified THF. Repeated recrystallization of the ZnTPP doped with IV or V was necessary to obtain suitable crystals. The crystals used to obtain the EPR spectra were approximately 3 × 1.5 × 1.5 mm.

The crystals were mounted with Dow silicone stopcock grease in a 3.5-mm segment of Wilmad synthetic quartz square cross section tubing (WQS-102, 2-mm i.d., 0.75-mm wall). A face of the holder was attached to the rod of a Varian E-229 one-cycle goniometer. For both IV and V two sets of data were obtained on two crystals obtained from the same solution with use of different methods of orienting the crystals. For one set of data (method A) the orientation of the crystal in the holder was adjusted iteratively to align the z axis of the silver **g** and **A** tensors with the rotation axis of the goniometer. Adjustment of the crystal orientation was continued until rotation through 180° caused little change in the overall spread of the silver lines and in the field position of the center of the silver lines. EPR spectra were collected at 15° intervals in this plane. The goniometer rod was then attached successively to the other two perpendicular faces of the holder, and data were collected as in the first plane. The accuracy of the rotation angles was indicated by the fact that in each plane spectra taken at 180° agreed with those at 0 ± 1°. The uncertainty in this method of orienting the crystal is greater for the silver complexes than for the previously examined copper and vanadyl complexes because of the small A anisotropy of the silver ion and the smaller nuclear spin. Subsequent simulation of the spectra indicated that the angle α between the silver z axis and the rotation axis of the goniometer z' (Figure 1A) was about 15° for the crystals of IV or V doped into ZnTPP.

A second set of data for each of the spin-labeled complexes (method B) was obtained by orienting the crystal in the holder such that the largest face of the crystal was perpendicular to the rotation axis of the goniometer and parallel to a face of the holder and the long axis of the crystal was parallel to a second face of the holder. EPR spectra were obtained at 15° intervals in this plane and in the two perpendicular planes defined by successively attaching the rod of the goniometer to the other two perpendicular faces of the holder. This is the same procedure that was used to orient the crystal of VO(TPP) doped into ZnTPP.[11] In that study it was found that the angles α and β (Figure 1A) were 33 and 55°, respectively. If the silver complexes IV and V had doped into ZnTPP with the same orientation of the porphyrin plane as had been observed for VO(TPP), the metal z axes (normal to the porphyrin plane) would have the same orientation relative to the crystal faces and the values of α and β would be the same. When the values of α and β obtained for VO(TPP) were used in the simulation of the spectra of IV and V doped into ZnTPP, the calculated orientation dependence of the g and A values was in good agreement with that observed in the experimental spectra. Thus, the orientation of the porphyrin planes in the host lattice is the same for the three systems. This observation is consistent with the previous conclusion that the orientations of the metal z axes for I, II, and III relative to the faces of the host crystal were similar.[10,11]

Computer Simulations

The perturbation calculation used in the simulation of the spectra is similar to that described previously for the analysis of powder EPR spectra of spin-labeled copper complexes[8] and single-crystal EPR spectra of spin-labeled copper and vanadyl complexes.[10,11] The Hamiltonian (eq 1) consists of terms for independent electrons 1 (silver)

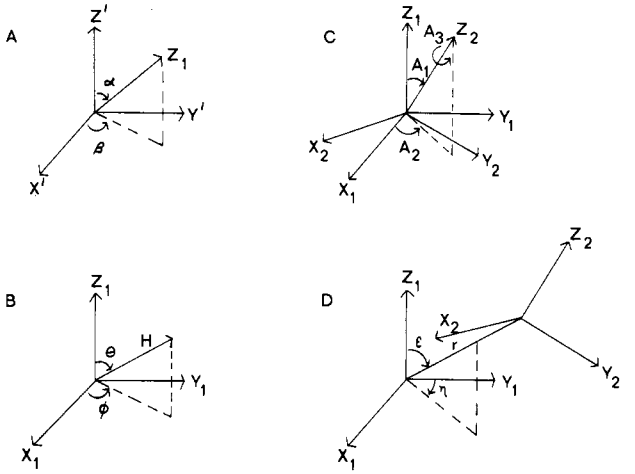

Figure 1. Definitions of the orientation relationships. (A) The angles α and β define the orientation of the silver z axis relative to the primed axes used for data collection. (B) The angles θ and ϕ define the orientation of the magnetic field relative to the axes of the silver electron. (C) The angles A_1, A_2, and A_3 define the orientation of the nitroxyl axes relative to the silver axes. (D) The angles ϵ and η define the orientation of the interspin vector r relative to the silver axes. Throughout the text r is used to denote the magnitude of the interspin vector.

$$\mathcal{H} = \mathcal{H}_1 + \mathcal{H}_2 + \mathcal{H}_{int} \quad (1)$$

$$\mathcal{H}_i = \sum_{j=x_i y_i z_i} (\beta g_j S_{ij} H_j + A_j S_{ij} I_{ij}) \qquad i = 1, 2 \quad (2)$$

$$\mathcal{H}_{int} = -JS_1 \cdot S_2 + \mathcal{H}_{dipolar} \quad (3)$$

and 2 (nitroxyl) as given in eq 2 and an interaction term as given in eq 3. The interaction term includes an isotropic exchange interaction and an anisotropic dipolar interaction. The symbols in eq 1–3 have their usual meanings and are discussed in detail in ref 6, 8, 10, and 15. The splitting between the singlet and triplet levels is J, and a negative value of J indicates an antiferromagnetic interaction. The angles that relate the orientation of the magnetic field to the axes of the silver electron are defined in Figure 1B. The angles that relate the orientation of the nitroxyl axes to the silver axes are defined in Figure 1C. The spectra of IV were sufficiently well resolved that it was possible to obtain approximate values for the angle A_3, which reflects the rotation of the nitroxyl x and y axes around the nitroxyl z axis. This angle was arbitrarily set equal to zero in previous calculations[8,10,11] and in the calculations of the spectra of V. The orientation of the interspin vector relative to the axes of the silver electron is defined in Figure 1D. In the following discussion r is used to denote the magnitude of the interspin vector and its orientation is defined by the angles ϵ and η.

For each set of data the orientation dependence of the nitrogen hyperfine splitting and of the electron–electron spin–spin splitting in the experimental (primed) axis systems was analyzed with the computer program ROTAN.[10] Examples of the agreement between the

(15) Smith, T. D.; Pilbrow, J. R. *Coord. Chem. Rev.* **1974**, *13*, 173–278.

Table II. Orientation and Interaction Parameters[a]

complex	species	A_1[d]	A_2[d]	A_3[d]	ϵ[d]	η[d]	r[b]	J[c]	% pop.	$d_\parallel$[c]
IV	1	172	84	90	120	−50	11.5	−33	16	−27
IV	2	70	28	0	102	−10	13.8	−26	34	−16
IV	3	172	84	0	115	−10	11.8	−35	34	−25
IV	4	172	84	90	107	39	13.0	−18	16	−19
V	1	55	50	0	46	−70	10.3	−6	20	−38
V	2	41	50	0	63	−25	12.0	5	20	−24
V	3	41	50	0	120	25	11.5	8	40	−27
V	4	41	50	0	34	60	9.5	−12	20	−49

[a] Parameters are defined in Figure 1. [b] In angstroms. [c] In units of 10^{-4} cm^{-1}. [d] In degrees.

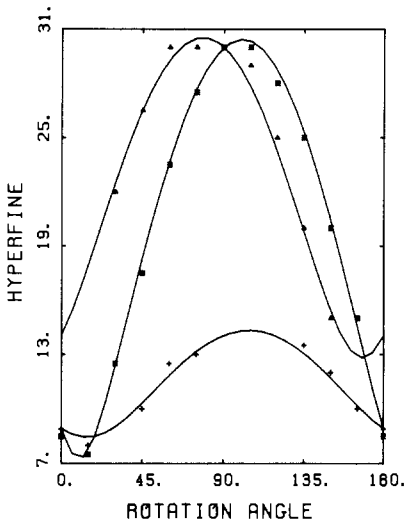

Figure 2. Plots of the orientation dependence of the nitroxyl nitrogen hyperfine splitting in gauss in three orthogonal planes for species 2 of trans isomer IV doped into ZnTPP. The crystal was oriented by method B. The experimental data are denoted by (▲) $x'y'$ plane, (■) $x'z'$ plane, and (+) $y'z'$ plane. The solid lines are the calculated curves.

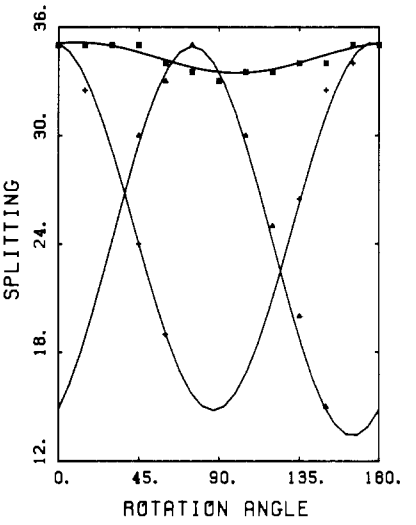

Figure 3. Plots of the orientation dependence of the spin–spin splitting in gauss in three orthogonal planes for species 2 of trans isomer IV doped into ZnTPP. The crystal was oriented by method B. The experimental planes are denoted by (▲) $x'y'$ plane, (■) $x'z'$ plane, and (+) $y'z'$ plane. The solid lines are the calculated curves.

experimental and calculated data are shown in Figures 2–4. The values of α and β were used to transform the values of A_1, A_2, ϵ, and η into the silver axis system. Because the silver g and A values were approximately axially symmetric (Table I), there was no molecular basis for a definition of the x and y axes. The angles η and A_2 given in Table II and used in the simulation of the spectra are relative to arbitrary x and y axes which were not the same for independent sets of data. Only the relative values can be used in comparisons. The EPR spectra were simulated with the program CRYST.[10]

Analysis of EPR Spectra

The EPR spectra that arise from weak electron–electron spin–spin interaction have been referred to as AB patterns[4,6,16] by analogy with high-resolution NMR.[17] As a result of the spin–spin interaction each of the hyperfine lines of each of the electrons is split into a doublet. For the spin-labeled silver complexes there are theoretically 216 silver lines and 216 nitroxyl lines in the spectrum if the splittings due to the silver nuclear spin for both silver isotopes, the nuclear spins of the porphyrin nitrogens, the nitroxyl nitrogen nuclear spin, and the electron–electron spin–spin interaction are included. It is assumed that only $\Delta m_I = 0$ transitions are observed. However, the splitting of the nitroxyl lines by the silver nuclear spin and by the nuclear spins of the porphyrin nitrogens was too small to be observed, so the nitroxyl portions of the spectra were apparent six-line patterns. Similarly the splitting of the silver lines by the nitroxyl nitrogen spin was too small to be observed so the silver portions of the spectra consisted of 36 lines. Since the hyperfine splitting by the porphyrin nitrogens was about the same magnitude as the silver nuclear hyperfine splitting, there was extensive overlap of the silver lines and it was difficult to visually identify AB patterns in the silver portions of the spectra. Therefore, the preliminary analysis of the spin–spin interaction in IV and V was based on the nitroxyl lines in the spectra. Computer simulation of the complete spectra indicated that the parameters obtained from the analysis of the nitroxyl lines were in good agreement with the observed splittings of the silver lines.

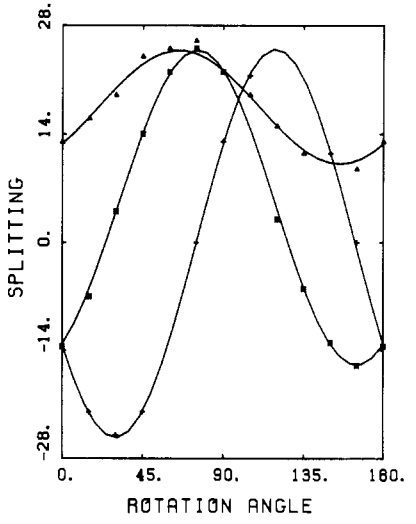

Figure 4. Plots of the orientation dependence of the spin–spin splitting in gauss in three orthogonal planes for species 1 of cis isomer V doped into ZnTPP. The crystal was oriented by method A. The experimental planes are denoted by (▲) $x'y'$ plane, (■) $x'z'$ plane, and (+) $y'z'$ plane. The solid lines are the calculated curves.

The number of lines in the nitroxyl regions of the spectra of IV and V indicated that more than one AB pattern was present. The orientation dependence of the silver lines indicated that the z axis of the silver **g** tensor had the same orientation for all the components of the spectra. Comparison of the spectra in three orthogonal planes

(16) Eaton, S. S.; DuBois, D. L.; Eaton, G. R. *J. Magn. Reson.* **1978**, *32*, 251–263.
(17) Abraham, R. J. "The Analysis of High Resolution NMR Spectra"; Elsevier: Amsterdam, 1971; Chapter 3.

showed that the multiple AB patterns did not result from sites that were related by rotation around the silver z axis or by reflection in the porphyrin plane. Thus, it was necessary to treat the spectra as the sum of contributions from species with different orientations of the interspin vector relative to the silver tensor and with different values of r and J.

For each of the crystals the assignment of the lines in the spectra to AB patterns was performed as previously reported for spin-labeled copper complexes I and II and vanadyl complex III.[10,11] In each of the crystals four distinguishable species were observed. At some orientations of the crystal additional weak lines were observed, which were not assigned. The lines were not resolved at enough orientations to adequately define them. It is possible that these lines are due to additional species with lower populations or broader lines or to interactions between two spin-labeled silver porphyrins as a result of imperfections in the doping of the host lattice. In all of the spectra a broad underlying spectrum was observed. The relative intensity of the signal varied between crystals. The g value of the signal had the same orientation dependence as the g value for the well-resolved silver lines, so it must be due to a species containing silver porphyrin that is doped into the crystal in the same orientation as the components giving the well-resolved lines. One possibility is that the doping is not completely random and that there are regions of the crystal in which there is interaction between several silver ions and several nitroxyls which give rise to a complex multispin spectrum.

For trans isomer IV the populations of species 2 and 3 were about twice those of species 1 and 4. The z axis of the nitroxyl nitrogen hyperfine tensor for species 2 was oriented differently than for species 1, 3, and 4, so the lines from species 2 could readily be distinguished from those of the other species at most orientations of the crystal. The nitroxyl lines from species 4 were generally sharper than the lines from species 1 and 3 and had smaller spin–spin splittings at most orientations of the crystal. The contributions to the spectra from species 1 and 3 were more difficult to distinguish because both gave rise to broad lines and large spin–spin splittings. However, at some orientations of the cyrstal it was possible to resolve two AB patterns arising from these two species. The populations of the species given in Table II are those obtained from the crystal that was oriented by method B. Although the same four species were observed in the crystal that was oriented by procedure A, the populations were slightly different. Species 4 was present in higher concentrations in the former crystal than in the latter, which facilitated the assignment of the lines for species 4. The variation in populations of sites in crystals grown under apparently identical conditions has also been noted in other studies.[18,19] Other parameters in Table II were obtained from the analysis of both sets of data for IV.

For cis isomer V, species 3 gave the prominent lines at most orientations of the crystal. The z axis of the nitroxyl nitrogen hyperfine tensor for species 1 was oriented differently than for the other species, which facilitated the assignment of its contributions to the spectra. The lines for species 2 and 4 were resolved at orientations where the spin–spin interaction for one was substantially different than for the other.

Approximate nitroxyl **g** and **A** tensors were obtained by diagonalization. The values were refined by comparison of calculated and experimental spectra at selected orientations of the crystals for which the spectra were well resolved. Due to the larger values of J observed for trans isomer IV than for the analogous complexes I–III and V, there was less overlap of the AB patterns and it was possible to analyze the nitroxyl g and A values in greater detail than in previous studies.[10,11] Species 1, 3, and 4 appeared to have about the same orientation of the z axis of the nitroxyl **g** and **A** tensors. The orientation dependence of the g and A values could only be matched by using slightly different principal values of the tensors for the four species and by making A_3 nonzero for species 1 and 4. There is considerable uncertainty in the values of A_3, but it is evident that the values are not the same for the four species. The principal values of the **g** and **A** tensors are listed in Table I. The orientation dependence of the nitrogen hyperfine splitting for species 2 is shown in Figure 2. The angles defining the orientation of the nitroxyl tensor are given in Table II. The spin–spin splittings for cis isomer V were smaller than for trans isomer IV so there was greater overlap of the AB patterns and it was not possible to analyze the **g** and **A** tensors in as great detail as for IV. The z axis of the nitroxyl was oriented similarly for species 2, 3, and 4. Small differences between the nitroxyl g and A values of the three species at a few orientations indicated that either the alignment of the nitroxyl tensors or the principal values of the tensors were not identical for all three species, but the differences were too small to adequately define. Hence, in the simulations it was assumed that the orientations of the nitroxyl hyperfine tensors and the principal values were the same for species 2, 3, and 4. Slightly different values were obtained for species 1. The results are summarized in Tables I and II. The g values for both IV and V are in good agreement with those observed previously for spin-labeled complexes I–III and for other piperidinyl nitroxyl radicals.[10,11]

The components of the **g** and **A** tensors for the silver electron were obtained by simulation of the spectra. Both ^{107}Ag and ^{109}Ag were included in the simulations although the contributions from the two isotopes were not resolved. The A values given in Table I are for ^{107}Ag. The values are in good agreement with literature values for a single crystal of AgTPP doped into H_2TPP, $g_\perp = 2.037$, $g_\parallel = 2.108$, $A_\perp = 28.3 \times 10^{-4}$ cm^{-1}, and $A_\parallel = 56.6 \times 10^{-4}$ cm^{-1} (effective averages for ^{107}Ag and ^{109}Ag),[20] and for AgTPP doped into ZnTPP(H_2O), $g_\perp = 2.037$, $g_\parallel = 2.108$, $^{107}A_\perp = 29.5 \times 10^{-4}$ cm^{-1}, $^{107}A_\parallel = 58 \times 10^{-4}$ cm^{-1}.[19] In the simulations it was assumed that the four porphyrin nitrogens were equivalent. However, since the z axis of the nitrogen hyperfine tensor is along the metal–nitrogen bond and the tensor is axially symmetric, the nitrogens are equivalent only at special orientations of the molecule. The differences between the couplings to the inequivalent nitrogens were too small to be resolved in the spectra. The difference should be greatest in the porphyrin plane. Ignoring this difference may account for some of the discrepancy between the observed and calculated silver lines. The components of the nitrogen hyperfine tensor were obtained from the apparent splittings by the method of Guzy et al.[21] The results that are given in Table I are in good agreement with values obtained from the ENDOR spectrum of AgTPP doped into ZnTPP(H_2O): $A_{xx}^N = 21.0 \times 10^{-4}$ cm^{-1}, $A_{yy}^N = 20.5 \times 10^{-4}$ cm^{-1}, $A_{zz}^N = 26.3 \times 10^{-4}$ cm^{-1}.[22]

The observed electron–electron spin–spin splittings were plotted as a function of the orientation of the crystal in the magnetic field. The values of ϵ, η, r, and J were adjusted until the calculated orientation dependence matched the experimental data. The plots in Figures 3 and 4 are typical of the agreement that was obtained. These plots are shown in the axis system used for data collection. The values given in Table II for the spin–spin interaction parameters are relative to the silver axes. The uncertainties in the parameters are as follows: angles, ±5°; r, ±0.5 A; J, $\pm 2 \times 10^{-4}$ cm^{-1}. The dipolar splittings calculated for the orientations of the crystal in which the magnetic field is parallel to the interspin vector ($d_\parallel$) are included in Table II.

Due to the extensive overlap of the lines in the spectra it was difficult to determine the line widths accurately. In the simulations it was assumed that the three lines of a nitroxyl hyperfine triplet had the same line width. However, at certain orientations of the crystal small differences (1–2 G) in the line widths of the three lines were observed. The appearance of the simulated spectra was strongly dependent on the line widths of the overlapping lines. Some of the discrepancy between observed and calculated spectra is due to differences in line widths for the three components of a nitroxyl triplet. For trans isomer IV species 2 and 4 had nitroxyl line widths between 2.5 and 6 G and species 1 and 3 had nitroxyl line widths between 4 and 14 G. Nitroxyl line widths for species 1–4 of cis isomer V were between 2 and 6 G. The silver line widths were between 6 and 12 G.

Results and Discussion

Figure 5 shows the spectrum of trans isomer IV obtained for $\theta = 18°$ and $\phi = 114°$. The major splittings of the silver lines were due to the porphyrin nitrogens (21 G). The g value for the silver lines was close to g_{zz} as expected for $\theta = 18°$. At this orientation 12 nitroxyl lines were clearly resolved. The zero-crossing points for the lines calculated for each of the

(18) Bohandy, J.; Kim, B. F.; Jen, C. K. *J. Magn. Reson.* **1974**, *15*, 420–426.
(19) Bohandy, J.; Kim, B. F. *J. Magn. Reson.* **1977**, *26*, 341–349.
(20) Manoharan, P. T.; Rogers, M. T. In "Electron Spin Resonance of Metal Complexes"; Yen, T. F., Ed.; Plenum Press: New York, 1969; pp 143–173.
(21) Guzy, C. M.; Raynor, J. B.; Symons, M. C. R. *J. Chem. Soc. A* **1969**, 2299–2303.
(22) Brown, T. G.; Hoffman, B. M. *Mol. Phys.* **1980**, *39*, 1073–1109.
(23) More, K. M.; Eaton, G. R.; Eaton, S. S. *Can. J. Chem.* **1982**, *25*, 1392–1401.

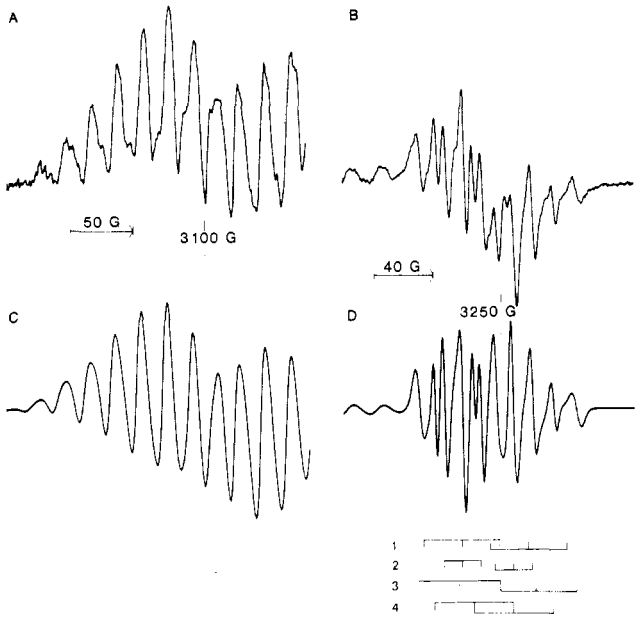

Figure 5. X-Band (9.108-GHz) EPR spectra of trans isomer IV doped into ZnTPP obtained at $\theta = 18°$ and $\phi = 114°$: (A) 240-G scan of the silver lines obtained with 2-G modulation amplitude and 5-mW microwave power; (B) 200-G scan of the high-field portion of the spectrum obtained with 0.63-G modulation amplitude and 5-mW microwave power. There is a 43-G overlap of the spectra in A and B. The overall amplification used for A is 10 times that for B. Parts C and D show the corresponding calculated spectra.

species are marked below the simulated spectrum. The nitroxyl nitrogen hyperfine splittings for species 1 and 3 were 27 G and the spin–spin splittings were 45 and 51 G, respectively, so there was extensive overlap of the lines from these two species. Only the lowest and highest field lines for these species were well resolved. The six lines from species 2 were all well resolved. The nitrogen hyperfine splitting for species 2 was 12 G, and the spin–spin splitting was 34 G. The nitrogen hyperfine splitting (26 G) for species 4 was approximately equal to the spin–spin splitting (27 G). Its spectrum was an apparent four-line pattern, which was also well resolved.

Figure 6 shows the EPR spectrum of trans isomer IV obtained for $\theta = 77°$ and $\phi = 70°$. The g value for the silver lines was close to $g_\perp$ as expected for $\theta = 77°$. The dominant splitting of the silver lines was due to the porphyrin nitrogens (24 G). The broad underlying signal was prominent at this orientation. No attempt was made in the simulations to match the broad underlying signal. Part of the silver spectrum is shown in Figure 6B at the same scale as that for the nitroxyl lines. The relative intensities of the sharp silver and nitroxyl lines were well matched by the simulated spectra. The zero-crossing points calculated for the nitroxyl lines for each of the species are indicated below the simulated spectrum. The nitrogen hyperfine splittings for species 1, 3, and 4 were about 10 G, and that for species 2 was 25 G. The spin–spin splitting for species 2 was 26 G, so it gave rise to the apparent four-line pattern that dominated the appearance of the spectrum. The spin–spin splittings from species 1, 3, and 4 were 46, 33, and 10 G, respectively. The large differences in these values permitted the detailed analysis of their respective contributions to the spectrum.

Figure 7 shows the EPR spectrum of cis isomer V obtained at $\theta = 168°$ and $\phi = 5°$. The g value of the silver electron was close to $g_\parallel$ as expected for $\theta = 168°$. The broad underlying signal was evident in the spectrum but was not as prominent as in the spectra of the crystals containing IV. The splitting of the silver lines was dominated by the porphyrin nitrogen hyperfine splitting (21 G). The zero-crossing points calculated

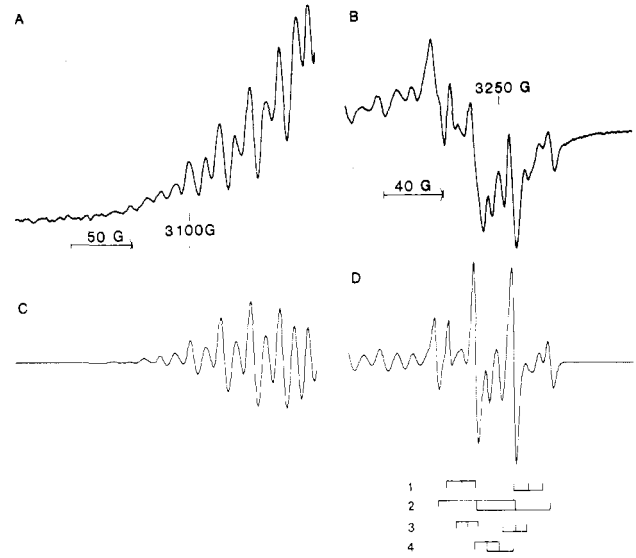

Figure 6. X-Band (9.106-GHz) EPR spectra of trans isomer IV doped into ZnTPP obtained at $\theta = 77°$ and $\phi = 69°$: (A) 240-G scan of the silver lines obtained with 2-G modulation amplitude and 5-mW microwave power; (B) 200-G scan of the high-field portion of the spectrum obtained with 0.63-G modulation amplitude and 5-mW microwave power. There is a 55-G overlap of the spectra in A and B. The overall amplification used for A is 5 times that for B. Parts C and D show the corresponding calculated spectra.

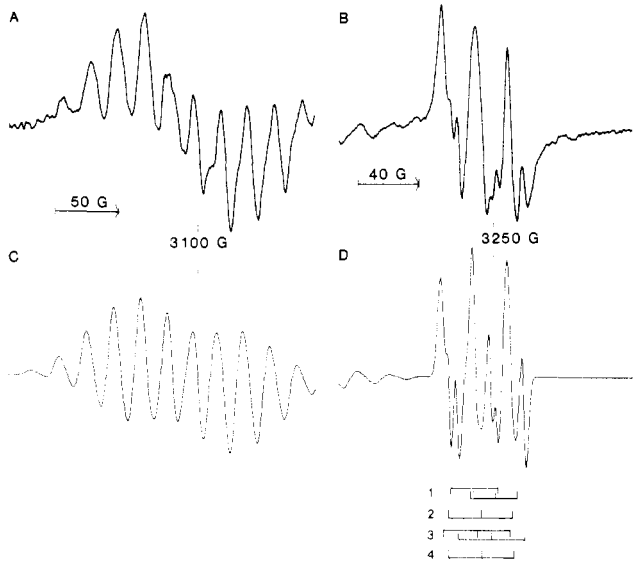

Figure 7. X-Band (9.106-GHz) EPR spectra of cis isomer V doped into ZnTPP obtained at $\theta = 168°$ and $\phi = 5°$: (A) 240-G scan of the silver lines obtained with 2-G modulation amplitude and 5-mW microwave power; (B) 200-G scan of the high-field portion of the spectrum obtained with 1-G modulation amplitude and 5-mW microwave power. There is a 42-G overlap of the spectra in A and B. The overall amplification used for A is 5.7 times that for B. Parts C and D show the corresponding calculated spectra.

for the nitroxyl lines of the four species are indicated below the simulated spectrum. The nitroxyl nitrogen hyperfine splitting was 16 G for species 1 and 21 G for species 2, 3, and 4. The spin–spin splitting for species 1 was 14 G. The low-field and high-field inner lines for this species were resolved. The other lines for species 1 were obscured by the lines from species 3. The spin–spin splittings for species 2 and 4 were small, so the signals were apparent three-line patterns. These lines were not well resolved at this orientation. The spin–spin splitting for species 3 was 9 G, so its spectrum was a six-line pattern. Since the population of species 3 is greater than the populations of the other species and its lines were relatively

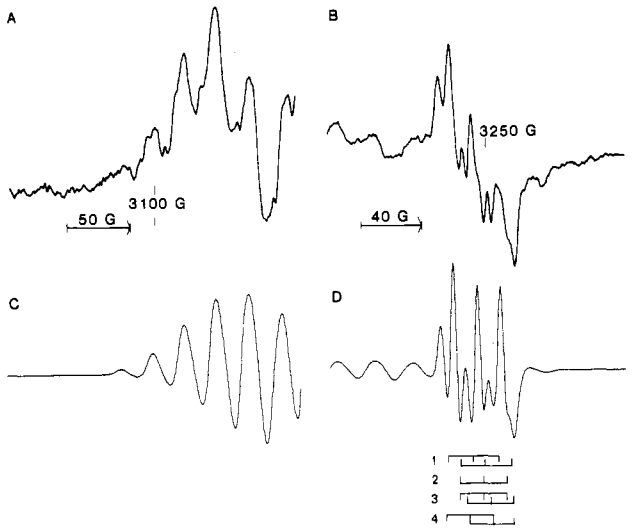

Figure 8. X-Band (9.109-GHz) EPR spectra of cis isomer V doped into ZnTPP obtained with $\theta = 102°$ and $\phi = 165°$: (A) 235-G scan of the silver lines obtained with 2-G modulation amplitude and 5-mW microwave power; (B) 200-G scan of the high-field portion of the spectrum obtained with 1-G modulation amplitude and 5-mW microwave power. There is a 23-G overlap of the spectra in A and B. The overall amplification used for A was 6 times that for B. Parts C and D show the corresponding calculated spectra.

sharp, its signal dominated the spectrum at this orientation.

Figure 8 shows the EPR spectrum of cis isomer V obtained at $\theta = 102°$ and $\phi = 165°$. The board underlying spectrum was clearly seen at this orientation and shifts the base line for both the silver and the nitroxyl portions of the spectrum. The silver g value was close to $g_\perp$ as expected for $\theta = 102°$. The zero-crossing points calculated for the nitroxyl lines for each of the species are indicated below the simulated spectrum. The nitroxyl nitrogen hyperfine splitting was 17 G for species 1 and 16 G for species 2, 3, and 4. The spin–spin splitting for species 1 was 8 G. The lowest and highest field lines for this species were resolved. The spin–spin splittings for species 2 and 3 were both small and gave rise to the dominant three-line pattern observed in the spectrum. The spin–spin splitting for species 4 was 16 G. The center two lines of the four-line pattern for this species were resolved.

When spin-labeled silver porphyrins IV or V are doped into the single crystal of ZnTPP, the spin-labeled side chain could be located at any of the eight pyrrole carbons and could be located above or below the porphyrin plane. Thus there are 16 possible locations for the substituent. Locations that are related by rotation around the silver z axis (normal to the plane) or by reflection in the porphyrin plane are distinguishable by EPR, but locations that are related by inversion are indistinguishable at all orientations of the crystal. Thus there are eight distinguishable locations. In the crystals of IV doped into ZnTPP three locations of the side chain were observed. For V doped into ZnTPP four locations were observed. The locations were characterized by different values of the parameter η. Since the side chains at the different orientations in the crystal gave rise to different values of η and of the spin–spin interaction parameters, they must be due to different species and not simply to different orientations in the crystal of identical species. We have arbitrarily chosen to keep the values of η between $\pm 90°$. However, it must be recognized that since the Hamiltonian is invariant to inversion the orientation $\epsilon = 120°$ and $\eta = -50°$ is indistinguishable from $\epsilon = 60°$ and $\eta = 130°$. Since the crystal structure of ZnTPP·THF has not been determined, the relationship between the molecular axes and the faces of the crystal is not known, so the definition of the x and y axes is arbitrary. Since the silver **g** and **A** tensors were approximately axial, there is also no

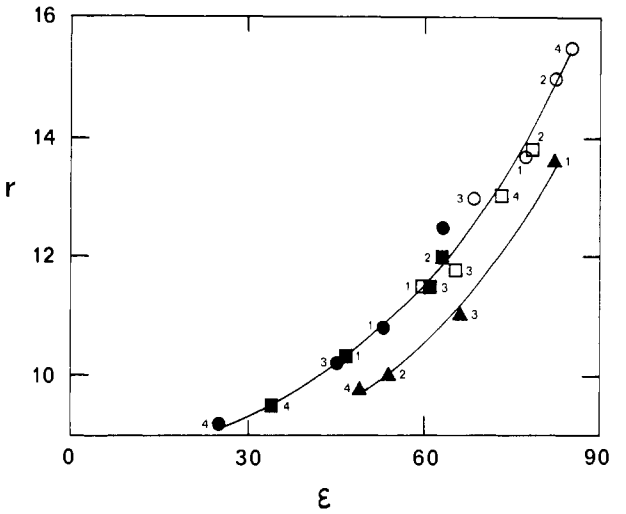

Figure 9. Plots of the values of r and ϵ observed for spin-labeled complexes I (○), II (●), III (▲), IV (□), and V (■). Each data point is labeled with the number of the species to which it refers.

molecular definition of the axes. The values of the orientation parameters are internally consistent for each of the molecules examined but do not permit a comparison of the values of η or A_2 for different crystals.

The values of η obtained for trans isomer IV were −50, −10, −10, and 39°. The 40–50° increments between the values of η are consistent with the angular increments expected for locations at successive pyrrole carbons around the porphyrin periphery as sketched in VI. The observation of two species

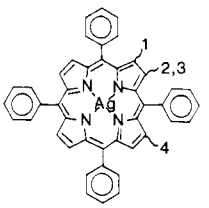

VI

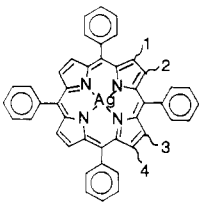

VII

with the same values of η indicates that there are two different conformations present at the same orientation or at inversion related orientations. For cis isomer V the values of η indicate that the four species may be viewed as sketched in VII.

The values of r for trans isomer IV ranged from 11.5 to 13.8 Å, and the values of ϵ ranged from 102 to 120°. In view of the inversion symmetry of the spectra the values of ϵ could also be viewed as ranging from 60 to 78°. For cis isomer V the values of r ranged from 9.5 to 12.0 Å and the values of ϵ were between 34 and 62°. In each case there was a correlation between the values of r and ϵ. Similar correlations were observed for complexes I–III.[10,11] The data for all five complexes are summarized in Figure 9. The values for the copper and silver complexes I, II, IV, and V all fall on a smooth curve. The values of r and ϵ tend to be smaller for the cis isomers than for the trans isomers, but there is some overlap. Inspection of molecular models suggests that as the spin-labeled side chain is forced toward the porphyrin plane, the values of r and ϵ both increase. The observed correlation may indicate that the different species arise from crystal-packing forces that force the bulky side chain toward the porphyrin plane to different extents for side chains at different locations around the porphyrin periphery. Further speculation on this question must await a crystal structure determination for the host. The data for the vanadyl complex III follow a pattern that is similar to that observed for the copper and silver complexes, but the curve is slightly offset. We have previously proposed that this offset may be due to preferential orientation of the side chains

Table III. Comparison of Values of J^a Obtained in Fluid Solution and Rigid Lattices

compd	M	isomer	J		
			fluid soln[b]	single cryst[c]	frozen soln[d]
I	Cu	trans	18-25[e]	−30 to −12[f]	−40[g]
II	Cu	cis	0-4[e]	−4 to +10[f]	<5[h]
III	VO	cis	<1[i]	−3 to +4[j]	<5[h]
IV	Ag	trans	33-44[i]	−35 to −18	−55[k]
V	Ag	cis	6-10[i]	−6 to +12	~10[k]

[a] In units of 10^{-4} cm^{-1}. If a sign is not given with the value, the sign is not known. [b] At room temperature in a variety of solvents. [c] Doped into ZnTPP. [d] Toluene–THF glass at ~−180 °C. [e] Reference 23. [f] Reference 10. [g] Reference 8. [h] Spin-spin splitting is less than the line width of the nitroxyl lines. [i] Reference 9. [j] Reference 11. [k] Reference 24.

on the same side of the porphyrin plane as the vanadyl oxygen.[11]

The values of J for both IV and V were found to vary significantly between species, indicating that the exchange interaction is highly sensitive to the detailed conformation of the linkage between the metal and the nitroxyl. However, the values in Table II indicate well-defined patterns. The values of J for trans isomer IV were consistently negative while the values for cis isomer V were smaller in magnitude and both positive and negative values were observed.

Table III includes all the data available for values of J obtained for complexes I–V in fluid solution, doped into ZnTPP, and in frozen toluene–THF glasses. For most of the complexes a range of values of J was observed in fluid solution and in the single crystals. Multiple contributions may also be present in the frozen solutions, but overlapping spectra are difficult to analyze because the components with sharper lines dominate the spectra.[8] The variations in the values of J reflect the dependence of the exchange interaction on the molecular conformation. These particular molecules are relatively rigid, so the variations were not large. For less rigid molecules changes in molecular conformation could cause differences between the values of J obtained under different conditions. In all three media the magnitude of the exchange interaction increased in the order $V^{IV}O$ < Cu(II) < Ag(II), which agrees well with other measures of spin delocalization.[9] For each of the complexes there is substantial agreement between the range of values of J observed in the three different media. For I and IV the magnitudes of the values of J obtained in frozen solution were somewhat larger than those obtained in the other media. The fluid-solution values presumably are the result of rapid averaging between molecular conformations with different values of J. The values of J for I in 9:1 toluene–THF solution increased from 24×10^{-4} cm^{-1} at 20 °C to 30×10^{-4} cm^{-1} at −60 °C.[24] Similarly the values of J for IV increased from 40×10^{-4} cm^{-1} at 20 °C to 51×10^{-4} cm^{-1} at −60 °C.[24] Thus, the values observed in frozen solution are in good agreement with the temperature dependence of the values observed in fluid solution. The smaller values of J in the single crystal indicate that the conformations of I and IV in that medium are not as favorable for exchange as those that are present in frozen solution. This may be due to steric constraints of the host lattice. Nevertheless the total range of values of J for either I or IV was only about a factor of 2. Since the values of J observed for cis isomers II, III, and V in the single crystal are both positive and negative, the small values observed in fluid solution may in part reflect rapid averaging of conformations with different signs of J.

Conclusions

Single-crystal EPR spectra of IV and V doped into ZnTPP indicated the presence of four conformations of each isomer in the crystal. The interspin distances were between 11.5 and 13.8 Å for IV and between 9.5 and 12.0 Å in V. The spin–spin coupling constant J was negative for trans isomer IV, but both positive and negative values of J were observed for cis isomer V. Comparison of the results obtained for complexes I–V in fluid solution, in ZnTPP single crystals, and in frozen solution indicated a substantial similarity in the values of J obtained for each complex in the three media. The combined data indicated that exchange increased in the order $V^{IV}O$ < Cu(II) < Ag(II) and cis < trans. These experiments clearly indicate that trends observed in fluid solution can be applied validly to similar systems in rigid matrices provided that the molecular geometry remains approximately constant.

Acknowledgment. This work was supported in part by NIH Grant No. GM21156.

Registry No. IV, 76438-03-4; V, 76497-29-5; ZnTPP, 14074-80-7.

(24) Eaton, S. S.; More, K. M.; Eaton, G. R., to be submitted for publication.